Neuronal nitric oxide synthase-induced S-nitrosylation of H-Ras inhibits calcium ionophore-mediated extracellular-signal-regulated kinase activity

Kimberly W. RAINES*, Guan-Liang CAO*†‡, Eun Kyoung LEE*, Gerald M. ROSEN*†‡ and Paul SHAPIRO*[1]

*Department of Pharmaceutical Sciences, University of Maryland School of Pharmacy, Baltimore, MD 21201, U.S.A., †Medical Biotechnology Center, University of Maryland Biotechnology Institute, Baltimore, MD 21201, U.S.A., and ‡Center for EPR Imaging for *In Vivo* Physiology, University of Maryland Biotechnology Institute, Baltimore, MD 21201, U.S.A.

nNOS (neuronal nitric oxide synthase) is a constitutively expressed enzyme responsible for the production of $NO^\bullet$ from L-arginine and O_2. $NO^\bullet$ acts as both an intra- and an inter-cellular messenger that mediates a variety of signalling pathways. Previous studies from our laboratory have demonstrated that nNOS production of $NO^\bullet$ blocks Ca^{2+}-ionophore-induced activation of ERK1/2 (extracellular-signal-regulated kinase 1/2) of the mitogen-activated protein kinases through a mechanism involving Ras G-proteins and Raf-1 kinase. Herein we describe a mechanism by which $NO^\bullet$ blocks Ca^{2+}-mediated ERK1/2 activity through direct modification of H-Ras. Ca^{2+}-mediated ERK1/2 activation in $NO^\bullet$-producing cells could be restored by exogenous expression of constitutively active mitogen-activated protein kinase kinase 1. In contrast, exogenous expression of constitutively active mutants of Raf-1 and H-Ras only partially restored ERK1/2 activity, by 50 % and 10 % respectively. On the basis

of these findings, we focused on $NO^\bullet$-mediated mechanisms of H-Ras inhibition. Assays for GTP loading and H-Ras interactions with the Ras-binding domain on Raf-1 demonstrated a decrease in H-Ras activity in the presence of $NO^\bullet$. We demonstrate that S-nitrosylation of H-Ras occurs in nNOS-expressing cells activated with Ca^{2+} ionophore. Mutation of a putative nitrosylation site at Cys^{118} inhibited S-nitrosylation and restored ERK1/2 activity by constitutively active H-Ras even in the presence of $NO^\bullet$. These findings indicate that intracellular generation of $NO^\bullet$ by nNOS leads to S-nitrosylation of H-Ras, which interferes with Raf-1 activation and propagation of signalling through ERK1/2.

Key words: extracellular-signal-regulated kinase (ERK), H-Ras, nitric oxide synthase (NOS), S-nitrosylation.

INTRODUCTION

$NO^\bullet$ is enzymatically formed by NOSs (nitric oxide synthases; EC 1.14.13.39), a family of three haem-containing enzymes, through the oxidation of L-arginine to $NO^\bullet$ and L-citrulline via the intermediate N^ω-hydroxy-L-arginine [1]. The three distinct isoforms of NOS are encoded by separate genes [2]: the constitutively expressed nNOS (neuronal NOS) [3] and eNOS (endothelial NOS) [4], and the endotoxin- or cytokine-inducible iNOS (inducible NOS) [5]. A distinctive property of the NOS enzymes is their ability to generate another free radical, superoxide ($O_2^{\bullet-}$) [6]. The ratio of $NO^\bullet$ to $O_2^{\bullet-}$ is dependent upon the concentration of the NOS substrate, L-arginine [6].

Not surprisingly, $NO^\bullet$ secreted from the different isoenzymes mediates a wide variety of regulatory functions. In the case of iNOS, a high level of $NO^\bullet$ production for prolonged periods is consistent with its role in host immunity [7]. In contrast, the rate of $NO^\bullet$ production by constitutively active eNOS or nNOS is at a much lower level, where $NO^\bullet$ is believed to be a transient cell-signalling agent [8]. One of the targets of $NO^\bullet$ generated by NOS is soluble guanylate cyclase, leading to increased cGMP. This second messenger regulates a wide variety of physiological functions, including vascular tone, platelet aggregation, inflammation, neurotransmission, learning and memory, penile erection, gastric emptying and hormone release [9].

Studies have also demonstrated that $NO^\bullet$ can react with cysteine residues of proteins to form S-nitrosothiols. S-nitrosylation has been shown to regulate the functions of a number of proteins, including activation of H-Ras [10], activation and inhibition of caspase 3 [11], inhibition of JNK (c-Jun N-terminal kinase) [12], inhibition of ornithine decarboxylase [13] and an increase in the affinity of oxygen for haemoglobin [14]. For example, direct modification at Cys^{118} by $NO^\bullet$ may be responsible for increases in H-Ras activity in Jurkat T-cells [10]. These findings indicate that this site of S-nitrosylation is critical for the redox regulation of H-Ras [15]. Moreover, S-nitrosylation of Cys^{118} on H-Ras has been suggested to trigger guanine nucleotide exchange, due, in part, to its surface location and accessibility [15]. Currently, we know that there is a consensus amino acid sequence for S-nitrosylation, namely K/R/H/D/E-C-D/E, which is present in a number of proteins, such as haemoglobin, cyclo-oxygenase and guanylate cyclase [16]. These findings indicate that S-nitrosylation is an important post-translational modification that regulates protein activity.

The MAPKs (mitogen-activated protein kinases) are major mediators of extracellular signals, which regulate cell functions such as proliferation, differentiation, migration, cell death and inflammatory responses [17]. MAPKs are serine/threonine kinases that include the ERKs (extracellular-signal-regulated kinases), JNKs and p38 MAPK [17]. Activation of the ERK1/2 pathway often

occurs in response to growth-factor stimulation of RTKs (receptor tyrosine kinases) and G-protein-coupled receptors, or through ion channels such as excitation of the NMDA (N-methyl-D-aspartate) glutamate receptor [17,18]. The RTK and NMDA receptors are coupled to the activation of Ras G-proteins through Src-homology-2-domain-containing proteins and guanine nucleotide-exchange factors, which are responsible for mediating the switch between the inactive Ras GDP-bound state to the active Ras GTP-bound form [17].

Previous research from our laboratory has demonstrated that the production of NO• by nNOS inactivates H-Ras and, subsequently, inhibits the downstream ERK1/2 proteins [19]. Understanding the mechanism by which NO• blocks this pathway could provide critical information pertinent to differential signalling by nNOS. In the present study, we have examined the mechanism by which NO• blocks Ca^{2+}-mediated ERK1/2 activity through modulation of Ras G-proteins. We have demonstrated that NO•-mediated inhibition of Ca^{2+}-induced ERK1/2 activity is due to S-nitrosylation of H-Ras at Cys^{118}, which disrupts activation of downstream events.

MATERIALS AND METHODS

Chemical and reagents

SDS and other electrophoresis reagents were purchased from Bio-Rad. DTT (dithiothreitol), MMTS (methyl methanethiosulphonate), L-NAME (N^{ω}-nitro-L-arginine methyl ester) hydrochloride, Hepes, EDTA, neocuproine, DMF (dimethylformamide), ascorbic acid, 2-mercaptoethanol, glutathione and GSNO (S-nitrosoglutathione) were obtained from Sigma–Aldrich.

Cell culture

Cell culture medium and supplements were obtained from Life Technologies, Invitrogen. N293 cells (HEK-293 transfected with nNOS) were obtained from Dr Yong Xia at Ohio State University, Columbus, OH, U.S.A. These cells were cultured in DMEM (Dulbecco's modified Eagle's medium) supplemented with 10 % (v/v) heat-inactivated fetal bovine serum, 50 μg/ml penicillin G and 50 μg/ml streptomycin at 37 °C in a 5 % CO_2, 95 % air-humidified incubator. Stable nNOS-expressing cells were maintained under selective pressure by treating the cells with 500 μg/ml Geneticin® at every fifth passage as described previously by Xia et al. [20]. HEK-293 cells were obtained from the A.T.C.C. (Manassas, VA, U.S.A.). To deplete intracellular stores of L-arginine from N293 and HEK-293 cells, the cells were initially cultured in complete medium for 2 days until 70–80 % confluent and then the medium was replaced with medium containing all the amino acids except L-arginine for 24 h as described previously [20]. To induce nNOS, the N293 cells were treated with the Ca^{2+} ionophore A23187 (C5149, Sigma–Aldrich) for the indicated incubation times. Inhibition of nNOS was achieved by incubating N293 cells with the NOS competitive inhibitor L-NAME (1 mM) for 24 h prior to Ca^{2+} ionophore activation. Cells were washed three times with cold PBS containing 0.9 mM $CaCl_2$ and 5.5 mM glucose, and then harvested in tissue lysis buffer, pH 7.4 [1 % (v/v) Triton X-100, 150 mM NaCl, 10 mM Tris/HCl, 1 mM EDTA, 1 mM EGTA, 0.2 mM sodium orthovanadate, 0.2 mM PMSF and 0.5 % (v/v) Nonidet P40] using a rubber scraper. Following lysis, the cells were centrifuged at 12 000 g for 10 min to remove insoluble material and the soluble proteins were analysed.

Cell transfections were performed as described previously [21] using 1 μg of plasmids containing cDNAs that express constitutively active mutants of MKK1 (MAPK kinase 1; provided by Dr Natalie Ahn, University of Colorado, Boulder, CO, U.S.A.), Raf-1 (Raf-1 BXB; provided by Dr Ulf Rapp, University of Wurzburg, Wurzburg, Germany) and H-Ras (H-Ras G12V; provided by Dr Melanie Cobb, University of Texas, Southwestern Medical Center, Dallas, TX, U.S.A.).

The murine macrophage cell line, RAW 264.7, was obtained from the A.T.C.C. (TIB-71). These cells were cultured in DMEM supplemented with 10 % heat-inactivated fetal bovine serum at 37 °C in a 5 % CO_2, 95 % air-humidified incubator. For experimental procedures, the cells were incubated with 100 ng/ml of LPS (lipopolysaccharide) for 18 h, and subjected to immunoblot analysis and the biotin-switch assay.

Nitrite assay

The accumulation of nitrite as a measure of NO• was determined spectrophotometrically after mixing 0.5 ml of each of culture medium and freshly prepared Griess reagent [0.1 % N-naphthyl-1-ethylenediamine in water and 1 % (w/v) sulphanilamide in 5 % phosphoric acid, mixed 1:1, v/v] [22]. Concentrations of nitrite were estimated by comparing absorbance readings at 550 nm against standard solutions of sodium nitrite prepared in the same media. The sensitivity limit of this assay is 0.5 μM. Aliquots (0.5 ml) of the culture medium were taken 2 h after Ca^{2+} ionophore stimulation.

S-nitrosylation measurements

The biotin-switch assay to measure S-nitrosylation was essentially performed as described previously [23]. Extracts were adjusted to 0.5 mg/ml protein as determined by the bicinchoninic acid assay (Pierce), and equal amounts of protein were blocked with 4 vol. of blocking buffer [225 mM Hepes, pH 7.7, 0.9 mM EDTA, 0.9 mM neocuproine, 2.5 % (w/v) SDS and 20 mM MMTS] at 50 °C for 20 min with agitation. After blocking, extracts were precipitated with acetone and resuspended in 0.1 ml HENS buffer [250 mM Hepes, pH 7.7, 1 mM EDTA, 0.1 mM neocuproine and 1 % (w/v) SDS] per mg of protein. At this point all operations are carried out in the dark. A one-third volume of a water-insoluble, thiol-reactive and cleavable biotin derivative, 4 mM N-[6-(biotinamido)hexyl]-3′-(2′-pyridyldithio)propionamide in DMF and 1 mM ascorbic acid was added, and incubated for 1 h at room temperature (25 °C). Proteins were acetone-precipitated again and resuspended in 0.1 ml HENS buffer before analysis by immunoblotting.

Immunoblot analysis

Cell protein lysates were diluted with an equal volume of 2× SDS/PAGE loading buffer and heated to 100 °C for 2 min. Total proteins (20 μg) were separated by SDS/PAGE (15 % gels) and transferred on to PVDF membranes. The immobilized proteins were then blocked in TBST (Tris-buffered saline containing 0.1 % Tween 20; 50 mM Tris/HCl, pH 7.5, 0.15 M NaCl and 0.1 % Tween 20) plus 5 % (w/v) non-fat dried milk. After overnight incubation at 4 °C with anti-ppERK1/2 (M8159, Sigma), anti-biotin (B7653, Sigma), anti-ERK2 (C-14, Santa Cruz Biotechnology) or anti-H-Ras (C-20, Santa Cruz Biotechnology) primary antibodies, the membranes were washed several times with TBST. The proteins were detected following incubation with horseradish-peroxidase-conjugated secondary antibody and detected using enhanced-chemiluminescence reagents purchased from PerkinElmer Life Sciences.

H-Ras activity assays

Protein lysates were cleared of insoluble material by centrifugation at 16 000 g for 20 min at 4 °C and then incubated for 2–4 h

with glutathione–Sepharose beads containing GST (glutathione S-transferase)–RBD (Ras-binding domain of Raf-1) as described previously [24]. Only active H-Ras in the GTP bound form will interact with the RBD. The Sepharose beads were washed three times with tissue lysis buffer, and bound proteins were eluted in $2 \times$ SDS/PAGE loading buffer. Proteins were resolved by SDS/PAGE (15 % gels) and analysed by immunoblotting for H-Ras.

To directly measure GTP loading, confluent HEK-293 and N293 cells in 60 mm $\times$ 15 mm cell-culture dishes were incubated in phosphate-free DMEM, pH 7.4, and 0.5 mCi carrier-free $[^{32}P]P_i$ (specific radioactivity 8500–9120 Ci/mmol; NEN/ PerkinElmer Life Sciences). After 4 h, the cells were treated with A23187 for up to 1 h or not treated. Cells were then gently washed with ice-cold PBS and lysed at 4 °C in 500 μl of lysis buffer. H-Ras protein was immunoprecipitated and incubated for 2 h with Protein G coupled to Sepharose 4B beads. The beads were collected by centrifugation at 10 000 g and washed once in tissue lysis buffer and twice in PBS before incubating for 20 min at 68 °C in 2 mM EDTA, 2 mM DTT, 0.2 % SDS, 0.5 mM GTP and 0.5 mM GDP, pH 7.5, to elute the radiolabelled GTP- and GDP-bound to H-Ras. Samples were applied to poly(ethyleneimine)-coated TLC plates in parallel with 100 nmol of GTP and GDP as unlabelled markers. After the nucleotides were separated in 1 M potassium phosphate buffer, pH 3.4, the plates were dried and exposed to X-Omat Blue XB-1 X-ray film (Kodak). The unlabelled markers GTP and GDP were visualized by UV light, and the areas of the TLC corresponding to ^{32}P-labelled GTP and GDP were quantified by PhosphorImaging (Storm840, Molecular Dynamics) using ImageQuant Software. The GTP/GDP ratios were determined by $[^{32}P]GTP$ divided by $([^{32}P]GTP + [^{32}P]GDP)$.

H-Ras C118S mutant generation

Using H-Ras G12V cDNA as a template, the C118S mutant was generated by PCR. The following primer sets were used, the first pair were used to generate the mutatuion and the second pair for subcloning and sequence verification: reverse mutagenic 5′-CT-TGTTCCCCACCAGCACCATGGGCACGTC-3′ and forward mutagenic 5′-GTGCTGGTGGGGAACAAGTCTGACCTGGC-TGCA-3′, and forward 5′-TGGCTAGCGTTTAAACTTA<u>AGC</u>-<u>TT</u>GGTAC-3′ (HindIII site is underlined) and reverse 5′-<u>CTC</u>-<u>GAG</u>TCTAGAGGGCCCGTTTAA-3′ (XhoI site is underlined). H-Ras G12V C118S was subcloned into the HindIII/XhoI sites of pcDNA3.1 (Invitrogen) and verified by sequencing, and the expressed protein was recognized by the anti-H-Ras monoclonal antibody.

Densitometry and statistical analysis

Immunoblot images were quantified by densitometry using NIH (National Institutes of Health) ImageJ software and AlphaEaseFC software for Windows. The results were expressed as means $\pm$ S.D. for at least three independent experiments. The means were compared using Student's t test, with $P < 0.05$ considered to be statistically significant.

RESULTS

ERK activation is dependent on L-arginine availability and NO• production

Previous reports have suggested that NO•, $O_2^{\bullet-}$ and H_2O_2 mediate a variety of biological responses through the MAPK signalling pathways [25–27]. It has also been documented that Ca^{2+} can
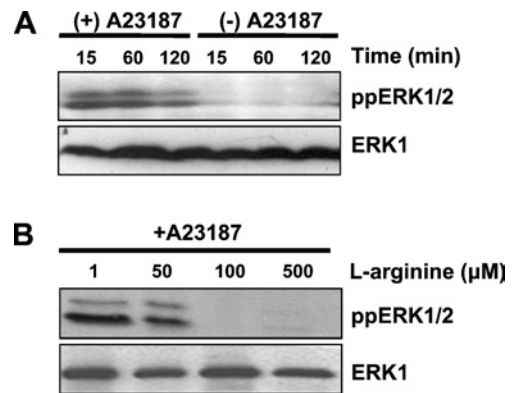

Figure 1   NOS regulation of ERK1/2 activity

(**A**) HEK-293 cells grown in normal growth medium were treated with or without 10 μM A23187 for 15 min to 2 h. Active ERK1/2 was assayed by immunoblot analysis using the anti-ppERK1/2 antibody. (**B**) N293 cells grown in medium containing various concentrations (1, 50, 100 or 500 μM) of L-arginine were treated with or without 10 μM A23187 for 2 h, and active ERK1/2 was analysed by immunoblotting using the anti-ppERK1/2 antibody. The results shown are representative of three independent experiments. Anti-ERK1 immunoblots are included as a protein loading control.

Table 1   NO• production is dependent on L-arginine levels

N293 cells grown with various concentrations (1, 50, 100 and 500 μM) of L-arginine were treated with 10 μM A23187 for 2 h. NO• production was then estimated from a portion of the growth medium that was subjected to the Griess reaction assay as outlined in the Materials and methods section. Results are means $\pm$ S.D. for three independent experiments.

[L-Arginine] (μM)	Nitrite (μM/h)
0	$0.09 + 0.01$
1	$1.10 + 0.10$
50	$4.51 + 0.41$
100	$5.77 + 0.52$
500	$7.16 + 0.64$

induce the ERK1/2 signalling pathway through activation of up-stream mediators [28]. Using N293 cells as a model, we have explored the importance of NO• in regulating ERK1/2 activation following Ca^{2+} ionophore stimulation of nNOS. In addition to activating nNOS, the Ca^{2+} ionophore A23187 is a useful agent for activating the ERK pathway [29]. Therefore nNOS effects on the ERK signalling pathway could be examined directly. Activation of ERK1/2 was estimated by immunoblotting for the phosphorylated forms of these proteins. For the control HEK-293 cells, treatment with the A23187-induced ERK1/2 activation, which was sustained for up to 1 h and decreased by 2 h (Figure 1A). However, stimulation of N293 cells with A23187 in the presence of increasing concentrations of L-arginine resulted in a dose-dependent decrease in A23187-induced ERK1/2 activation (Figure 1B).

Next, the correlation between NO• production by the N293 cells and the concentration of L-arginine in the culture medium was explored. There was no evidence of NO• production in the medium of A23187-stimulated N293 cells cultured in DMEM that did not contain L-arginine (Table 1). However, as the concentration of L-arginine increased, detectable levels of NO• were observed (Table 1). This finding, in conjunction with the results presented in Figure 1(B), indicates that NO• generation at a rate of $\geqslant 2$ μM/h inhibits ERK1/2 phosphorylation.
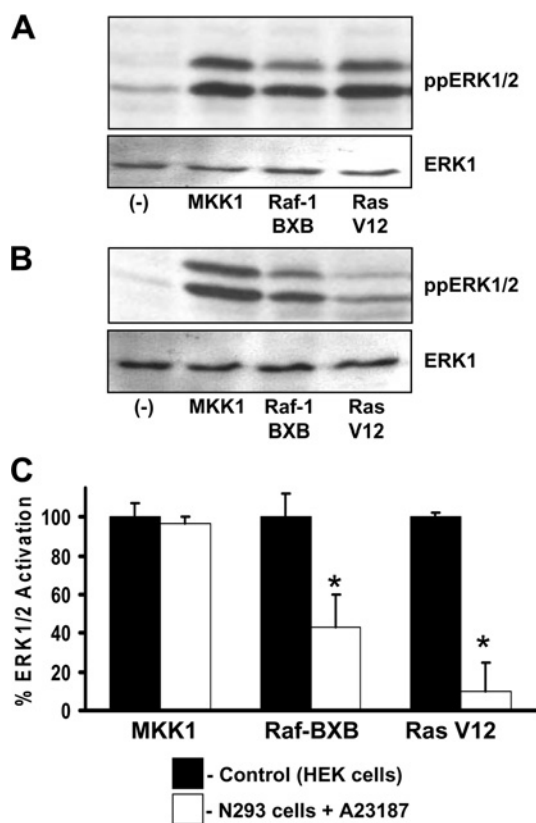
Figure 2   NO• inhibition of ERK1/2 activity is primarily through H-Ras

(**A**) Control HEK-293 cells were transfected with constitutively active MKK1, Raf-1 (Raf-1 BXB) or H-Ras (Ras V12) mutant constructs and grown under normal growth conditions for 24–48 h. The upper and lower panels show immunoblots of ppERK1/2 and total ERK1 respectively. (**B**) N293 cells were transfected with constitutively active MKK1, Raf-1 or H-Ras mutant constructs and were grown under normal growth conditions. Cells were stimulated with 10 μM A23187 and harvested 2 h later. The upper and lower panels show immunoblots for ppERK1/2 and total ERK1 respectively. (**C**) Ratio of ppERK1/2 to total ERK1 as determined by densitometry. Data represent the means $\pm$ S.D. for three independent experiments. * $P < 0.05$.

Recovery of ERK1/2 activity by constitutively active upstream proteins

The mechanisms of NO•-mediated inhibition of Ca^{2+} ionophore-induced ERK1/2 activity were studied in N293 cells transfected with constitutively active mutants of MKK1, Raf-1 (Raf-BXB) or H-Ras (H-Ras G12V) (see the Materials and methods section for details). As controls, HEK-293 cells transfected with constitutively active mutants of MKK1, Raf-1 or H-Ras showed similar activation of ERK1/2 (Figure 2A). In N293 cells stimulated to produce NO•, ERK1/2 activation by A23187, which normally is inhibited, could be fully recovered by co-expression of constitutively active MKK1 (Figures 2B and 2C). However, the expression of constitutively active Raf-1 or H-Ras only restored ERK activity to approx. 50 % or 10 % respectively compared with the control HEK-293 cells (Figures 2B and 2C). These results suggest that NO• can block ERK1/2 activation by direct or indirect inhibition of H-Ras and/or partial inhibition of Raf-1 protein activity.

NO• inhibits constitutively active H-Ras

To examine further the mechanism of NO•-mediated inhibition of H-Ras, we determined whether activation of nNOS had a direct
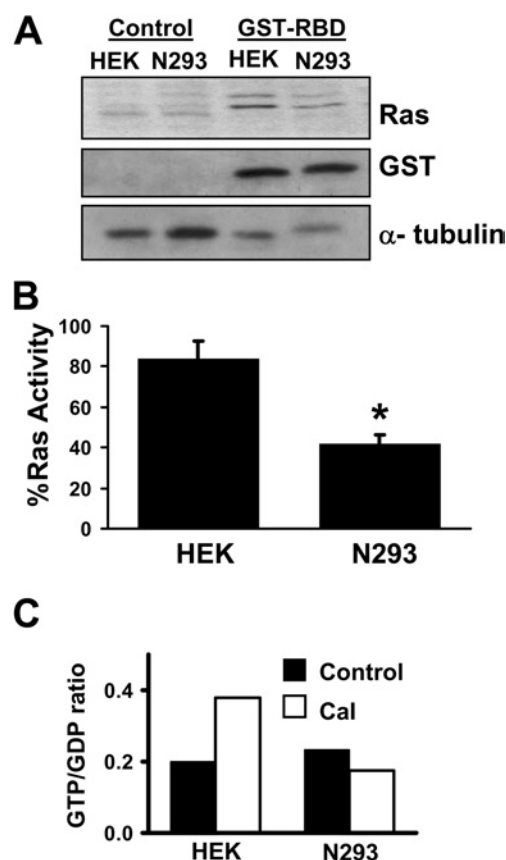

Figure 3   NO• inhibits H-Ras activity

(**A**) HEK-293 (HEK) or N293 cells were treated with 10 μM A23187 for 2 h. Cell lysates were subjected to the H-Ras pull-down assay using GST–RBD. GST–RBD protein complexes were separated by SDS/PAGE (15 % gels) and immunoblotted for H-Ras or GST. An anti-α-tubulin immunoblot from the initial lysates was included as a protein loading control. (**B**) The relative amount of active H-Ras co-interacting with GST–RBD was quantified by densitometry. Results are means $\pm$ S.D. for three independent experiments. * $P < 0.05$. (**C**) HEK-293 (HEK) and N293 cells were incubated in DMEM medium containing 0.5 mCi of carrier-free [^{32}P]P$_i$ for 4 h. The cells were then stimulated with 10 μM A23187 for 1 h, lysed and then immunoprecipitated for 2 h at 4 °C with anti-H-Ras antibody. H-Ras-bound nucleotides (GTP and GDP) were eluted and separated by TLC. GTP/GDP ratios were quantified by PhosphorImaging. The data represent the means for two independent experiments. The GTP/GDP ratios for the two experiments were 0.13 and 0.27 for HEK-293 control cells; 0.45 and 0.31 for HEK-293 cells plus A23187 (labelled Cal); 0.21 and 0.26 for N293 cells; and, 0.17 and 0.18 for N293 cells plus A23187 (labelled Cal).

affect on H-Ras activity. To test this, HEK-293 and N293 cells were transfected with H-Ras G12V and then treated with A23187. The samples were incubated with or without GST–RBD, and the bound H-Ras was estimated by immunoblot analysis. Since the interactions between H-Ras and the RBD are dependent on active H-Ras in its GTP-bound form, this method is an acceptable indicator of H-Ras activity [24]. As indicated in the N293 cells, the generation of NO• decreased the amount of H-Ras interacting with GST–RBD, whereas control HEK-293 cells showed elevated levels of H-Ras interacting with GST–RBD (Figures 3A and 3B). These results suggest that NO• blocks H-Ras signalling to ERK1/2 by directly inhibiting H-Ras activity (e.g. decreased GTP loading) or by preventing interactions with the Raf-1 protein.

To determine whether NO• directly inhibits H-Ras activity through inhibition of GTP loading, we directly measured H-Ras loaded with guanine nucleotides. HEK-293 and N293 cells incubated with [^{32}P]P$_i$ were activated with A23187 and H-Ras was
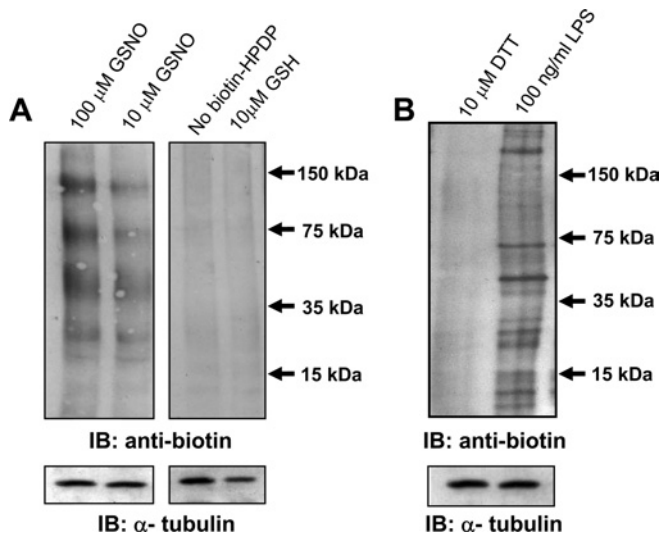
Figure 4   S-nitrosylation of proteins detected by the biotin-switch assay

(**A**) Left-hand panel: N293 cells were incubated with 100 μM and 10 μM GSNO for 1 h and subjected to the S-nitrosylation assay (see the Materials and methods section). Right-hand panel: N293 cells were treated with 10 μM GSNO but not treated with biotin–HPDP or the control compound glutathione, followed by analysis of S-nitrosylation. In these samples only the endogenous biotinylated proteins are detectable. (**B**) S-nitrosylation was measured in RAW 264.7 macrophage cells treated with the iNOS inducer LPS (100 ng/ml) or the reducing agent DTT (10 μM). The expression of α-tubulin is included as a protein loading control. The results shown are representative of three independent experiments. IB, immunoblot.

immunoprecipitated with anti-H-Ras antibody. ^{32}P-labelled guanine nucleotides were eluted from the H-Ras and separated on poly(ethyleneimine)-coated TLC plates. The radiolabelled GTP and GDP were identified by comparing their mobility with unlabelled GTP and GDP standards, and quantified by Phosphor-Imaging. As shown in Figure 3(C), increased H-Ras GTP loading was observed in HEK-293 cells treated with A23187, in contrast, N293 cells treated with A23187 showed no change in H-Ras GTP loading. As expected, and similar to Figure 1, ERK activation in these samples was observed in HEK-293 cells treated with A23187, but not N293 cells (results not shown). These findings indicate that H-Ras GTP loading is inhibited in NO$^\bullet$-generating cells.

Analysis of S-nitrosylation in protein lysates

To explore the mechanisms of NO$^\bullet$ inhibition of H-Ras, we took advantage of previous studies that suggested the H-Ras protein was post-translationally modified by NO$^\bullet$ through S-nitrosylation of cysteine residues [15]. Whether this mechanism is operative in the N293 cells was examined using the S-nitrosylation biotin-switch assay, which was first used in the detection and identification of nitrosylated proteins in brain extracts [23] and primary endothelial cells [30]. N293 cells treated with A23187 were incubated with GSNO, a reagent that can *trans*-nitrosylate available cysteine residues. The biotin-switch assay involves three sequential steps for identifying nitrosylation: (i) blockage of cellular free thiols by MMTS; (ii) specific reduction of S-nitrosothiols to free thiols by ascorbic acid; and (iii) labelling of free thiols with a specific biotin derivative. The biotin-switch assay was performed and the resulting biotinylated proteins were detected by immunoblot analysis (Figure 4A). Endogenous biotinylated proteins are shown in GSNO-treated lanes (Figure 4A, left-hand panel). Although very feint bands appear in samples treated in the

absence of biotin–HDPD or with the reducing agent glutathione (Figure 4A, right-hand panel), biotinylation of proteins is clearly increased with increasing concentrations of GSNO (10–100 μM). Thus, in agreement with other cell models, this method is able to detect an increase in nitrosylation in N293 cells.

To validate that the S-nitrosylation assay would also detect NO$^\bullet$-mediated nitrosylation generated by endogenous NOS, we examined RAW 264.7 murine macrophage cells stimulated with LPS, which is known to cause induction of iNOS expression and the production of NO$^\bullet$ [31]. RAW 264.7 cells were treated with LPS or, as a control, the reducing agent DTT. Following the biotin-switch assay and immunoblot analysis, LPS induced S-nitrosylation of a number of proteins, revealing that this method is viable for detecting enzyme-mediated S-nitrosylation events (Figure 4B).

NOS-mediated S-nitrosylation of H-Ras

To determine whether S-nitrosylation events were controlled by nNOS activation, we used the L-arginine analogue L-NAME, which is an inhibitor of NOS activity. N293 cells were grown to confluence and incubated with 1 mM L-NAME for 18 h before A23187 stimulation. The cells were lysed and the biotin-switch assay was performed. This was followed by immunoprecipitation of H-Ras and immunoblot analysis of the biotinylated proteins. In the absence of L-NAME, strong biotin reactivity with a protein corresponding to the molecular mass of H-Ras specifically indicated S-nitrosylation of H-Ras (Figure 5A). However, in the presence of L-NAME, no detectable biotin reactivity was observed at the H-Ras molecular mass, indicating the absence of S-nitrosylation (Figure 5A). In addition, no biotin reactivity was observed in the absence of A23187 treatment (results not shown). These findings lend further support to the conclusion that S-nitrosylation of H-Ras is mediated by nNOS activity.

Cys^{118} of H-Ras mediates NO$^\bullet$-induced inhibition of ERK1/2

It has previously been confirmed by NMR that NO$^\bullet$ modification of the H-Ras protein occurs at Cys^{118} [32]. In this experiment, we introduced a C118S mutation in the constitutively active H-Ras G12V protein to test whether S-nitrosylation at this site mediated NO$^\bullet$ inhibition of ERK1/2. N293 cells were transfected with wild-type H-Ras, H-Ras G12V or H-Ras G12V C118S mutants and examined for ERK1/2 activity with and without A23187 stimulation. In the absence of A23187, H-Ras G12V and the H-Ras G12V C118S mutants showed similar activation of ERK1/2 (Figure 5B). Thus the addition of the C118S mutation did not appear to affect the constitutive H-Ras activity. However, unlike the inhibition of ERK1/2 activity that was observed in nNOS cells expressing H-Ras G12V, A23187 induction of NO$^\bullet$ production had no effect on ERK1/2 activity in cells expressing the H-Ras G12V C118S mutant (Figure 5B).

Lastly, we compared the levels of H-Ras S-nitrosylation in cells expressing wild-type H-Ras, H-Ras G12V or H-Ras G12V C118S. As shown in Figure 5(C), N293 cells expressing wild-type H-Ras, H-Ras G12V or the H-Ras V12 C118S mutant showed little or no detectable levels of nitrosylation in the absence of A23187. In contrast, A23187 treatment to induce NO$^\bullet$ production resulted in increased S-nitrosylation of both wild-type H-Ras or H-Ras V12 mutants (Figure 5C); however, S-nitrosylation of the H-Ras V12 (C118S) mutant was significantly inhibited compared with H-Ras V12 and wild-type H-Ras (Figures 5C and 5D). This finding indicates that Cys^{118} participates in the nNOS-generated NO$^\bullet$-mediated S-nitrosylation of the H-Ras protein.
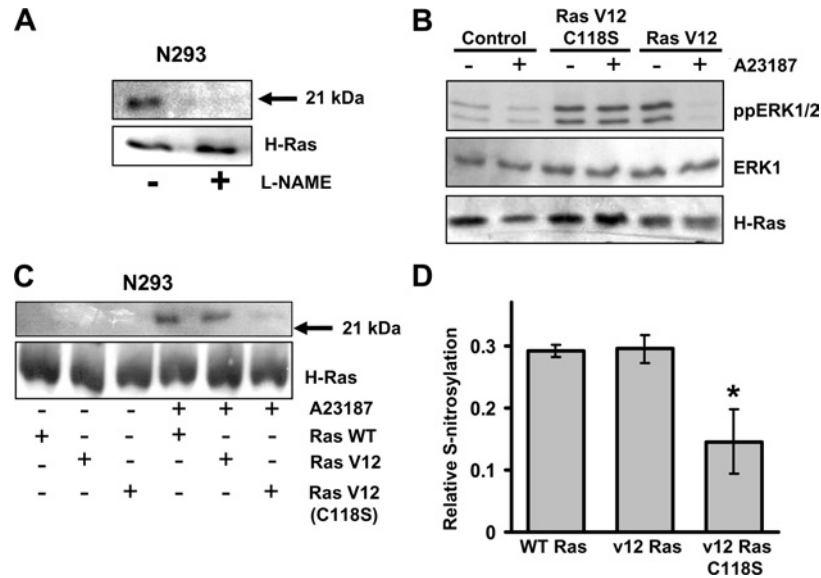
Figure 5   NOS-mediated S-nitrosylation of H-Ras

(**A**) N293 cells were incubated in the presence or absence of 1 mM L-NAME for 18 h before the addition of 10 μM A23187. Cells were lysed and subjected to the S-nitrosylation assay followed by immunoprecipitation of H-Ras. The resulting biotinylated proteins were detected by immunoblot analysis with an anti-biotin antibody. Total H-Ras expression is included as a protein loading control. The results shown are representative of two independent experiments. (**B**) N293 cells expressing wild-type H-Ras, constitutively active H-Ras (Ras V12) or H-Ras G12V C118S (Ras V12 C118S) were treated with or without 10 μM A23187 for 2 h. Cell lysates were immunoblotted for active ERK1/2 (ppERK1/2), total ERK1 or H-Ras in the top, middle, and bottom panels respectively. The results shown are one representative of three independent experiments. (**C**) N293 cells transfected with wild-type H-Ras, H-Ras G12V (Ras V12), or H-Ras G12V C118S [Ras V12 (C118S)] were treated with or without 10 μM A23187 for 2 h. Following S-nitrosylation analysis using the biotin-switch assay, H-Ras was immunoprecipitated, and immunoblotted using anti-biotin and anti-H-Ras antibodies. The results shown are representative of three independent experiments. (**D**) The relative amount of S-nitrosylated H-Ras was quantified by densitometry. Results are means $\pm$ S.D. for three independent experiments. * $P < 0.05$. WT, wild-type.

DISCUSSION

In the present study, we have demonstrated that NO$^\bullet$ can directly modify H-Ras at Cys[118] by S-nitrosylation, which subsequently leads to inhibition of signalling through the ERK pathway. Whereas activation of nNOS with A23187 completely blocked ERK activation by a constitutively active H-Ras mutant (H-Ras G12V), ERK activity was partially blocked or not blocked at all by constitutively active mutants of Raf-1 or MKK1 respectively. We have shown that replacement of Cys[118] with a serine residue restored the ability of active H-Ras to stimulate the ERK pathway in the presence of NO$^\bullet$. From these findings, we propose that S-nitrosylation of Cys[118] on H-Ras is sufficient to block oncogenically mutated H-Ras activity and disrupt activation of Raf-1 and the MKK/ERK pathway (Figure 6).

Although the present paper focuses on H-Ras regulation, we cannot exclude the possibility that S-nitrosylation also regulates Raf-1 activity. The constitutively active Raf-1 mutant used in the present study is a truncated protein, consisting of the Raf-1 kinase catalytic domain that lacks the N-terminal regulatory domain [33]. However, future studies will be needed to identify potential S-nitrosylation sites in the Raf-1 regulatory and catalytic domains, and also to determine their functional significance. Importantly, our studies utilized a cell model where we can manipulate the production of intracellular NO$^\bullet$ by nNOS. We believe that this model more accurately represents the physiological interactions between intracellular NO$^\bullet$ and signalling proteins compared with studies that have manipulated NO$^\bullet$ levels through the use of exogenous NO$^\bullet$ donors [19], where the rate of NO$^\bullet$ production is uncertain and undoubtedly much greater than the rate of cellular-derived NO$^\bullet$ production from NOS.

H-Ras contains five cysteine residues of which at least four, at positions 118, 181, 184 and 186, have been shown to be modified
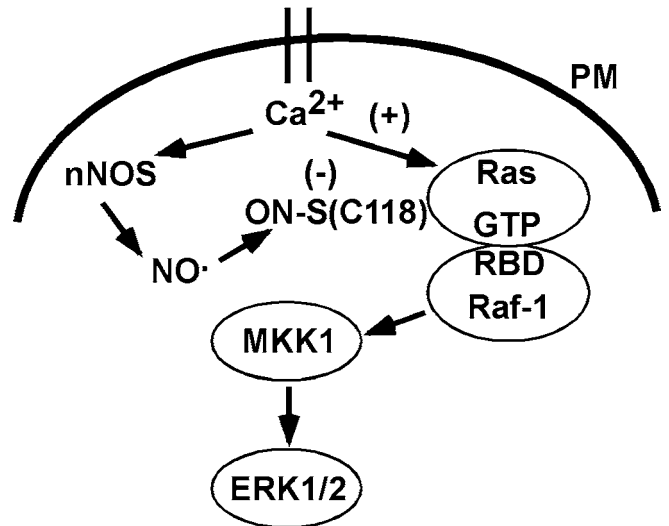

Figure 6   Model of nNOS mediated S-nitrosylation of H-Ras and inhibition of ERK1/2 activation

Upon activation of nNOS by calcium influx through the plasma membrane (PM), increased NO$^\bullet$ levels can lead to S-nitrosylation of proximal proteins such as H-Ras. S-nitrosylation of H-Ras on Cys[118] may diminish H-Ras activation of Raf-1, possibly by affecting the interactions between a RBD on Raf-1, which is adjacent to GTP binding site and Cys[118] of H-Ras. The structure of H-Ras and the RBD was previously reported by Zeng et al. [50] and adapted to this model.

through S-nitrosylation [34]. Given that Cys[181] and Cys[184] are palmitoylated and Cys[186] is farnesylated, and that all three residues are involved in targeting H-Ras to the plasma membrane, it is intriguing to hypothesize that post-translational modification

through S-nitrosylation could regulate H-Ras activity by altering membrane targeting. Previous studies suggest that Cys^{118} is the primary residue targeted by S-nitrosylation that affects H-Ras function [15]. In agreement with our findings, previous studies have reported that S-nitrosylation inhibits both neuronal cell growth [35] and H-Ras activation of the ERK pathway in mouse fibroblasts [36]. Moreover, it has been suggested that vascular smooth-muscle cells treated with $NO^•$, supplied by exposure to $NO^•$ donors such as sodium nitroprusside, show inhibition of epidermal growth factor-mediated Ras activation of Raf-1 [37].

In contrast, previous studies examining the role of oxidative stress in the MAPK pathway have demonstrated increased H-Ras activity in response to S-nitrosylation in human umbilical vein endothelial cells [38] or exposure to H_2O_2 in NIH3T3 and PC12 cells [39]. In addition, endothelial cells may require $NO^•$ to mediate vascular endothelial growth factor induction of cell proliferation through the Ras/ERK pathway [40]. In T-lymphocytes treated with the $NO^•$ donor sodium nitroprusside, Cys^{118} was identified as the critical S-nitrosylation site responsible for H-Ras activation of the ERK pathway [15]. As one possible mechanism, it was suggested that S-nitrosylation of Cys^{118} activates H-Ras by increasing or mimicking GTP exchange [15]. Cys^{118} is also an important S-nitrosylation site as it is located on an exposed loop that contacts the guanine nucleotide (Figure 6) [41]. However, our results (Figures 3–5) suggest that $NO^•$ inhibits GTP loading of H-Ras in cells. A recent study using purified H-Ras protein indicated that $NO^•$ on its own had no effect on GTP loading [42].

Other studies have also suggested that the function of S-nitrosylation at Cys^{118} is not to regulate H-Ras activity directly, but to affect H-Ras regulation of downstream targets. For example, a H-Ras C118S mutant could be activated in a similar manner compared with wild-type H-Ras by nerve growth factor in PC12 cells, suggesting that GTP loading of H-Ras in the C118S mutant was not altered [43]. Interestingly, cells expressing the H-Ras C118S mutant demonstrated a higher susceptibility for apoptosis compared with cells expressing wild-type H-Ras after 7 days in the presence of nerve growth factor, indicating that S-nitrosylation of H-Ras may be involved in sustaining signalling pathways that are essential for the survival in this differentiated neuronal cell model [43]. As such, this study reported that S-nitrosylation may protect cell survival by promoting H-Ras activation of survival signalling pathways regulated by phosphatidylinositol 3-kinases [43].

A variety of signalling proteins have been identified as targets for S-nitrosylation [44]. The consequence of $NO^•$ production combined with S-nitrosylation has been actively studied in the context of promoting or inhibiting apoptosis [45]. S-nitrosylation has been suggested to inhibit JNK activity, which promotes apoptotic responses to stimuli such as interferon-γ [46]. Moreover, $NO^•$ may suppress apoptosis by inhibiting caspase 3 through S-nitrosylation [11]. In contrast, S-nitrosylation of the cell-survival kinase Akt on Cys^{224} may lead to Akt inactivation and support a role for $NO^•$ in enhancing the apoptotic response [47].

One explanation for the differential effects of S-nitrosylation on protein function may be related to the level of $NO^•$ in each study. S-nitrosylation of proteins is directly correlated with $NO^•$ concentration [48]. Whereas the flux of $NO^•$ generated from stimulation of nNOS-containing cells is low, in the order of picomoles, manipulation of $NO^•$ levels through the use of extracellular donors undoubtedly supplies $NO^•$ at much higher rates. Thus the differences in the source and amount of $NO^•$ available to S-nitrosylate may directly influence the effect $NO^•$ has on intracellular signalling.

The understanding of alternative (e.g. cGMP-independent) mechanisms for cell signalling regulation by $NO^•$ will be important for characterizing the diverse roles that $NO^•$ appears to play in regulating a myriad of physiological functions. The role of free radicals in the direct modification and regulation of MAPKs and their biological functions is largely undefined. Since H-Ras is an oncogene product, that is known to be mutated in many different types of tumours [49], the understanding of its regulation by $NO^•$ may shed light on H-Ras modulation of downstream signalling pathways that are involved in cellular transformation.

REFERENCES

1   Moncada, S. and Higgs, A. (1993) The L-arginine–nitric oxide pathway. N. Engl. J. Med. **329**, 2002–2012

2   Forstermann, U., Schmidt, H. H., Pollock, J. S., Sheng, H., Mitchell, J. A., Warner, T. D., Nakane, M. and Murad, F. (1991) Isoforms of nitric oxide synthase: characterization and purification from different cell types. Biochem. Pharmacol. **42**, 1849–1857

3   Xu, W., Gorman, P., Sheer, D., Bates, G., Kishimoto, J., Lizhi, L. and Emson, P. (1993) Regional localization of the gene coding for human brain nitric oxide synthase (NOS1) to 12q24.2–24.31 by fluorescent in situ hybridization. Cytogenet. Cell Genet. **64**, 62–63

4   Marsden, P. A., Heng, H. H., Scherer, S. W., Stewart, R. J., Hall, A. V., Shi, X. M., Tsui, L. C. and Schappert, K. T. (1993) Structure and chromosomal localization of the human constitutive endothelial nitric oxide synthase gene. J. Biol. Chem. **268**, 17478–17488

5   Chartrain, N. A., Geller, D. A., Koty, P. P., Sitrin, N. F., Nussler, A. K., Hoffman, E. P., Billiar, T. R., Hutchinson, N. I. and Mudgett, J. S. (1994) Molecular cloning, structure, and chromosomal localization of the human inducible nitric-oxide synthase gene. J. Biol. Chem. **269**, 6765–6772

6   Pou, S., Keaton, L., Surichamorn, W. and Rosen, G. M. (1999) Mechanism of superoxide generation by neuronal nitric-oxide synthase. J. Biol. Chem. **274**, 9573–9580

7   Akaike, T. and Maeda, H. (2000) Nitric oxide and virus infection. Immunology **101**, 300–308

8   Finkel, T. (1998) Oxygen radicals and signalling. Curr. Opin. Cell Biol. **10**, 248–253

9   Lane, P. and Gross, S. S. (1999) Cell signalling by nitric oxide. Semin. Nephrol. **19**, 215–229

10 Lander, H. M., Ogiste, J. S., Pearce, S. F., Levi, R. and Novogrodsky, A. (1995) Nitric oxide-stimulated guanine nucleotide exchange on p21ras. J. Biol. Chem. **270**, 7017–7020

11 Rossig, L., Fichtlscherer, B., Breitschopf, K., Haendeler, J., Zeiher, A. M., Mulsch, A. and Dimmeler, S. (1999) Nitric oxide inhibits caspase-3 by S-nitrosation in vivo. J. Biol. Chem. **274**, 6823–6826

12 Hall, J. P., Merithew, E. and Davis, R. J. (2000) c-Jun N-terminal kinase (JNK) repression during the inflammatory response? Just say NO. Proc. Natl. Acad. Sci. U.S.A. **97**, 14022–14024

13 Bauer, P. M., Buga, G. M., Fukuto, J. M., Pegg, A. E. and Ignarro, L. J. (2001) Nitric oxide inhibits ornithine decarboxylase via S-nitrosylation of cysteine 360 in the active site of the enzyme. J. Biol. Chem. **276**, 34458–34464

14 Jia, L., Bonaventura, C., Bonaventura, J. and Stamler, J. S. (1996) S-nitrosohaemoglobin: a dynamic activity of blood involved in vascular control. Nature (London) **380**, 221–226

15 Lander, H. M., Hajjar, D. P., Hempstead, B. L., Mirza, U. A., Chait, B. T., Campbell, S. and Quilliam, L. A. (1997) A molecular redox switch on p21ras. Structural basis for the nitric oxide–p21ras interaction. J. Biol. Chem. **272**, 4323–4326

16 Stamler, J. S., Toone, E. J., Lipton, S. A. and Sucher, N. J. (1997) (S)NO signals: translocation, regulation, and a consensus motif. Neuron **18**, 691–696

17 Lewis, T. S., Shapiro, P. S. and Ahn, N. G. (1998) Signal transduction through MAP kinase cascades. Adv. Cancer Res. **74**, 49–139

18 Sheng, M. and Kim, M. J. (2002) Postsynaptic signalling and plasticity mechanisms. Science **298**, 776–780

19 Raines, K. W., Cao, G. L., Porsuphatana, S., Tsai, P., Rosen, G. M. and Shapiro, P. (2004) Nitric oxide inhibition of ERK1/2 activity in cells expressing neuronal nitric-oxide synthase. J. Biol. Chem. **279**, 3933–3940

20 Xia, Y., Dawson, V. L., Dawson, T. M., Snyder, S. H. and Zweier, J. L. (1996) Nitric oxide synthase generates superoxide and nitric oxide in arginine-depleted cells leading to peroxynitrite-mediated cellular injury. Proc. Natl. Acad. Sci. U.S.A. **93**, 6770–6774

21 Cha, H., Lee, E. K. and Shapiro, P. (2001) Identification of a C-terminal region that regulates mitogen-activated protein kinase kinase-1 cytoplasmic localization and ERK activation. J. Biol. Chem. **276**, 48494–48501

22 Green, L. C., Wagner, D. A., Glogowski, J., Skipper, P. L., Wishnok, J. S. and Tannenbaum, S. R. (1982) Analysis of nitrate, nitrite, and [^{15}N]nitrate in biological fluids. Anal. Biochem. **126**, 131–138

23 Jaffrey, S. R., Erdjument-Bromage, H., Ferris, C. D., Tempst, P. and Snyder, S. H. (2001) Protein S-nitrosylation: a physiological signal for neuronal nitric oxide. Nat. Cell Biol. **3**, 193–197

24 de Rooij, J. and Bos, J. L. (1997) Minimal Ras-binding domain of Raf1 can be used as an activation-specific probe for Ras. Oncogene **14**, 623–625

25 Andreka, P., Zang, J., Dougherty, C., Slepak, T. I., Webster, K. A. and Bishopric, N. H. (2001) Cytoprotection by Jun kinase during nitric oxide-induced cardiac myocyte apoptosis. Circ. Res. **88**, 305–312

26 Ingram, A. J., James, L., Thai, K., Ly, H., Cai, L. and Scholey, J. W. (2000) Nitric oxide modulates mechanical strain-induced activation of p38 MAPK in mesangial cells. Am. J. Physiol. Renal Physiol. **279**, F243–F251

27 Zhang, B., Hirahashi, J., Cullere, X. and Mayadas, T. N. (2003) Elucidation of molecular events leading to neutrophil apoptosis following phagocytosis: cross-talk between caspase 8, reactive oxygen species, and MAPK/ERK activation. J. Biol. Chem. **278**, 28443–28454

28 Enslen, H., Tokumitsu, H., Stork, P. J., Davis, R. J. and Soderling, T. R. (1996) Regulation of mitogen-activated protein kinases by a calcium/calmodulin-dependent protein kinase cascade. Proc. Natl. Acad. Sci. U.S.A. **93**, 10803–10808

29 Atherfold, P. A., Norris, M. S., Robinson, P. J., Gelfand, E. W. and Franklin, R. A. (1999) Calcium-induced ERK activation in human T lymphocytes. Mol. Immunol. **36**, 543–549

30 Martinez-Ruiz, A. and Lamas, S. (2004) Detection and proteomic identification of S-nitrosylated proteins in endothelial cells. Arch. Biochem. Biophys. **423**, 192–199

31 Chi, D. S., Qui, M., Krishnaswamy, G., Li, C. and Stone, W. (2003) Regulation of nitric oxide production from macrophages by lipopolysaccharide and catecholamines. Nitric Oxide **8**, 127–132

32 Williams, J. G., Pappu, K. and Campbell, S. L. (2003) Structural and biochemical studies of p21 Ras S-nitrosylation and nitric oxide-mediated guanine nucleotide exchange. Proc. Natl. Acad. Sci. U.S.A. **100**, 6376–6381

33 Heidecker, G., Huleihel, M., Cleveland, J. L., Kolch, W., Beck, T. W., Lloyd, P., Pawson, T. and Rapp, U. R. (1990) Mutational activation of c-raf-1 and definition of the minimal transforming sequence. Mol. Cell. Biol. **10**, 2503–2512

34 Mallis, R. J., Buss, J. E. and Thomas, J. A. (2001) Oxidative modification of H-ras: S-thiolation and S-nitrosylation of reactive cysteines. Biochem. J. **355**, 145–153

35 Hess, D. T., Patterson, S. I., Smith, D. S. and Skene, J. H. (1993) Neuronal growth cone collapse and inhibition of protein fatty acylation by nitric oxide. Nature (London) **366**, 562–565

36 Baker, T. L., Booden, M. A. and Buss, J. E. (2000) S-nitrosocysteine increases palmitate turnover on Ha-Ras in NIH 3T3 cells. J. Biol. Chem. **275**, 22037–22047

37 Yu, S. M., Hung, L. M. and Lin, C. C. (1997) cGMP-elevating agents suppress proliferation of vascular smooth muscle cells by inhibiting the activation of epidermal growth factor signalling pathway. Circulation **95**, 1269–1277

38 Lander, H. M., Jacovina, A. T., Davis, R. J. and Tauras, J. M. (1996) Differential activation of mitogen-activated protein kinases by nitric oxide-related species. J. Biol. Chem. **271**, 19705–19709

39 Guyton, K. Z., Liu, Y., Gorospe, M., Xu, Q. and Holbrook, N. J. (1996) Activation of mitogen-activated protein kinase by H_2O_2: role in cell survival following oxidant injury. J. Biol. Chem. **271**, 4138–4142

40 Oliveira, C. J., Schindler, F., Ventura, A. M., Morais, M. S., Arai, R. J., Debbas, V., Stern, A. and Monteiro, H. P. (2003) Nitric oxide and cGMP activate the Ras-MAP kinase pathway-stimulating protein tyrosine phosphorylation in rabbit aortic endothelial cells. Free Radical Biol. Med. **35**, 381–396

41 Pai, E. F., Krengel, U., Petsko, G. A., Goody, R. S., Kabsh, W. and Wittinghofer, A. (1990) Refined crystal structure of the triphosphate conformation of H-ras p21 at 1.35 Å resolution: implications for the mechanism of GTP hydrolysis. EMBO J. **9**, 2351–2359

42 Heo, J. and Campbell, S. L. (2006) Ras regulation by reactive oxygen and nitrogen species. Biochemistry **45**, 2200–2210

43 Teng, K. K., Esposito, D. K., Schwartz, G. D., Lander, H. M. and Hempstead, B. L. (1999) Activation of c-Ha-Ras by nitric oxide modulates survival responsiveness in neuronal PC12 cells. J. Biol. Chem. **274**, 37315–37320

44 Stamler, J. S., Lamas, S. and Fang, F. C. (2001) Nitrosylation: the prototypic redox-based signalling mechanism. Cell **106**, 675–683

45 Chung, H. T., Pae, H. O., Choi, B. M., Billiar, T. R. and Kim, Y. M. (2001) Nitric oxide as a bioregulator of apoptosis. Biochem. Biophys. Res. Commun. **282**, 1075–1079

46 Park, H. S., Huh, S. H., Kim, M. S., Lee, S. H. and Choi, E. J. (2000) Nitric oxide negatively regulates c-Jun N-terminal kinase/stress-activated protein kinase by means of S-nitrosylation. Proc. Natl. Acad. Sci. U.S.A. **97**, 14382–14387

47 Yasukawa, T., Tokunaga, E., Ota, H., Sugita, H., Martyn, J. A. and Kaneki, M. (2005) S-nitrosylation-dependent inactivation of Akt/protein kinase B in insulin resistance. J. Biol. Chem. **280**, 7511–7518

48 Zhang, Y., Keszler, A., Broniowska, K. A. and Hogg, N. (2004) Characterization and application of the biotin-switch assay for the identification of S-nitrosated proteins. Free Radical Biol. Med. **38**, 874–881

49 Bos, J. L. (1989) ras oncogenes in human cancer: a review. Cancer Res. **49**, 4682–4689

50 Zeng, J., Nheu, T., Zorzet, A., Catimel, B., Nice, E., Maruta, H., Burgess, A. W. and Treutlein, H. R. (2001) Design of inhibitors of Ras–Raf interaction using a computational combinatorial algorithm. Protein Eng. **14**, 39–45